Supplementary Information to:

Dishevelled is a NEK2 substrate controlling dynamics of centrosomal linker proteins

by

Igor Cervenka, Jana Valnohova, Ondrej Bernatik, Jakub Harnos, Matej Radsetoulal, Katerina Sedova, Katerina Hanakova, David Potesil, Miroslava Sedlackova, Alena Salasova, Zachary Steinhart, Stephane Angers, Gunnar Schulte, Ales Hampl, Zbynek Zdrahal, Vitezslav Bryja

Contains:

- **Supplementary Figures S1-S6**
- **Supplementary Tables S1-S5**
- **Supplementary Methods**

Supplementary Figures

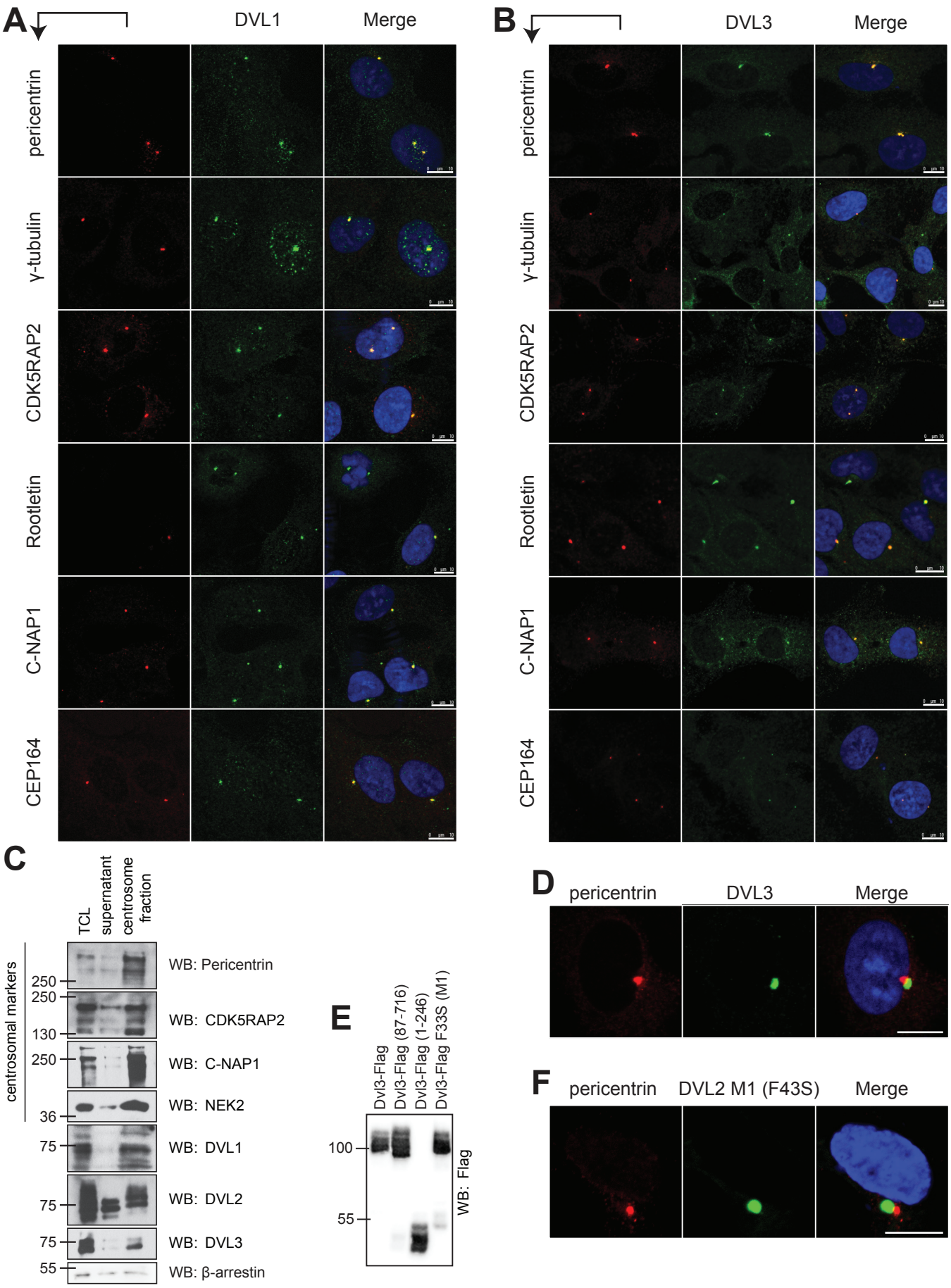

Figure S1. Centrosomal localization of Dishevelled. (A, B) Co-localization of Dishevelled with centrosome components (red) in RPE cells was assessed by immunofluorescence. All tested proteins co-localize with endogenous Dishevelled 1 and 3 (green). (C) Centrosomal fraction was isolated from HEK293 cells and immunoblotted with antibodies against centrosomal proteins, DVL isoforms and β-arrestin as control. (D) Co-localization of endogenous Dishevelled with pericentrin (red) in HEK293 cell assessed by immunofluorescence. (E) Expression levels of DVL3 mutants used in Fig. 1 assessed by western blotting. (F) HEK293 cells were transfected with low amount of DVL2 M1 (F33S) and co-localization with pericentrin (red) was assessed. Despite not being able to polymerize and activate Wnt signaling DVL2 M1 still co-localizes to centrosome. DAPI (blue). Scale bars: 10 μm.

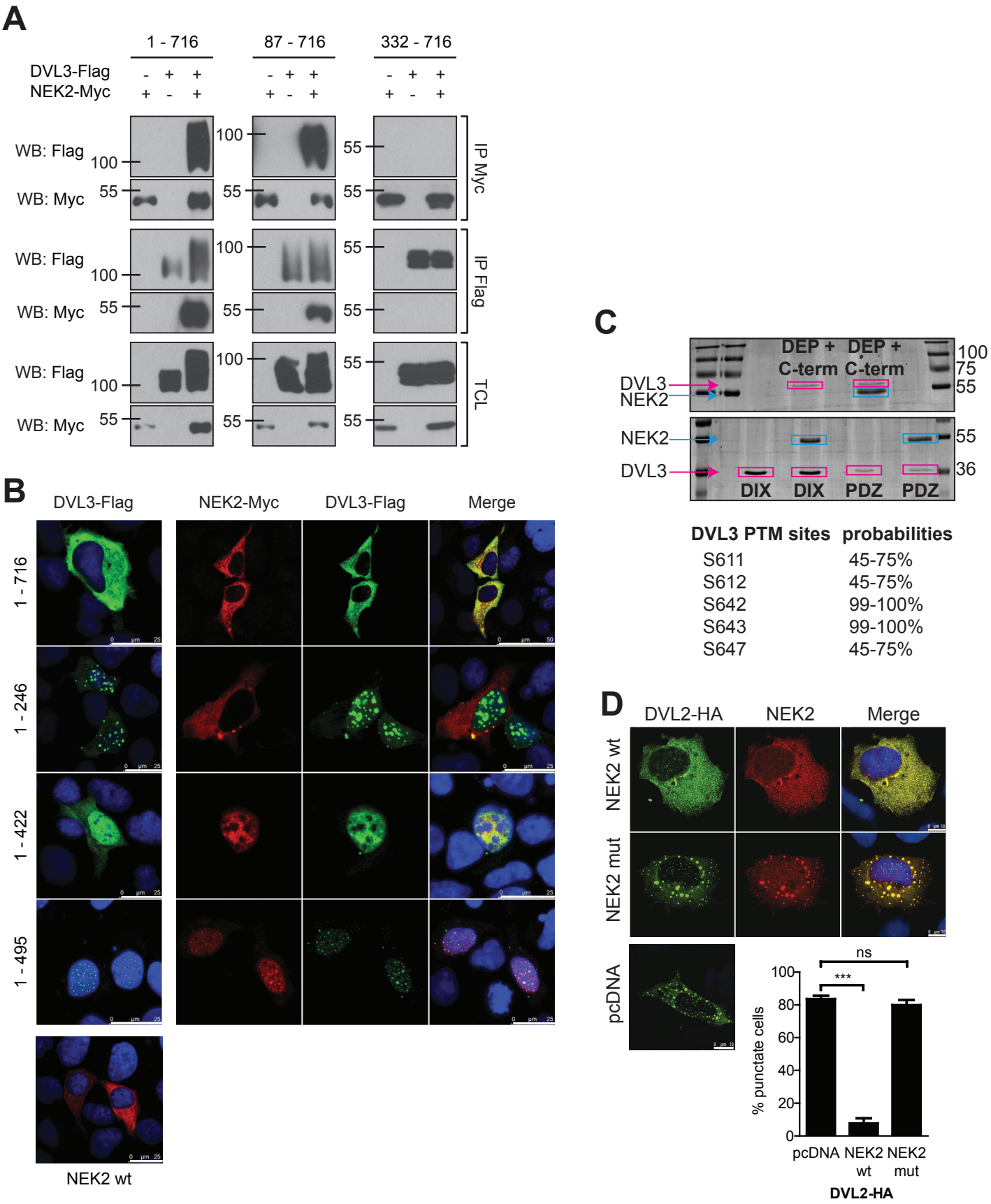

Figure S2. Characterization of the interaction between DVL3 and NEK2. (A) DVL3 deletion mutants truncated from N-terminus (DVL3 87-716 and DVL3 332-716) were co-immunoprecipitated with wild-type NEK2 kinase in HEK293 cells. Only constructs containing PDZ domain show binding and electrophoretic mobility shift. (B) DVL3 deletion mutants truncated from C-terminus (DVL3 1-246, DVL3 1-422, DVL3 1-495) (green) were co-transfected with wild-type NEK2 (red) kinase in HEK293 cells, and localization was assessed by immuno-fluorescence. Exclusively cytoplasmic localization of NEK2 is drastically changed to nuclear when co-expressed with PDZ domain containing DVL mutants. (C) SDS-PAGE gel of in vitro kinase assay using NEK2 (200 ng) and recombinant GST-tagged DIX, PDZ or DEP-C terminus domain respectively of DVL3 as substrates (50 ng). After Coomassie staining of the gel, phosphorylation was detected by MS/MS. (D) DVL (green) shows localization change from punctate to cytoplasmic even after co-expression of wild-type NEK2 (red), but not after co-expression of mutant NEK2 (red). Graph summarizes percentage of cells with punctate appearance of DVL. Graphs represent mean ±SEM of three independent replicates. *** $P < 0.001$; (ANOVA - Bonferroni's posttest). DAPI (blue), scale bars: 10 µm.

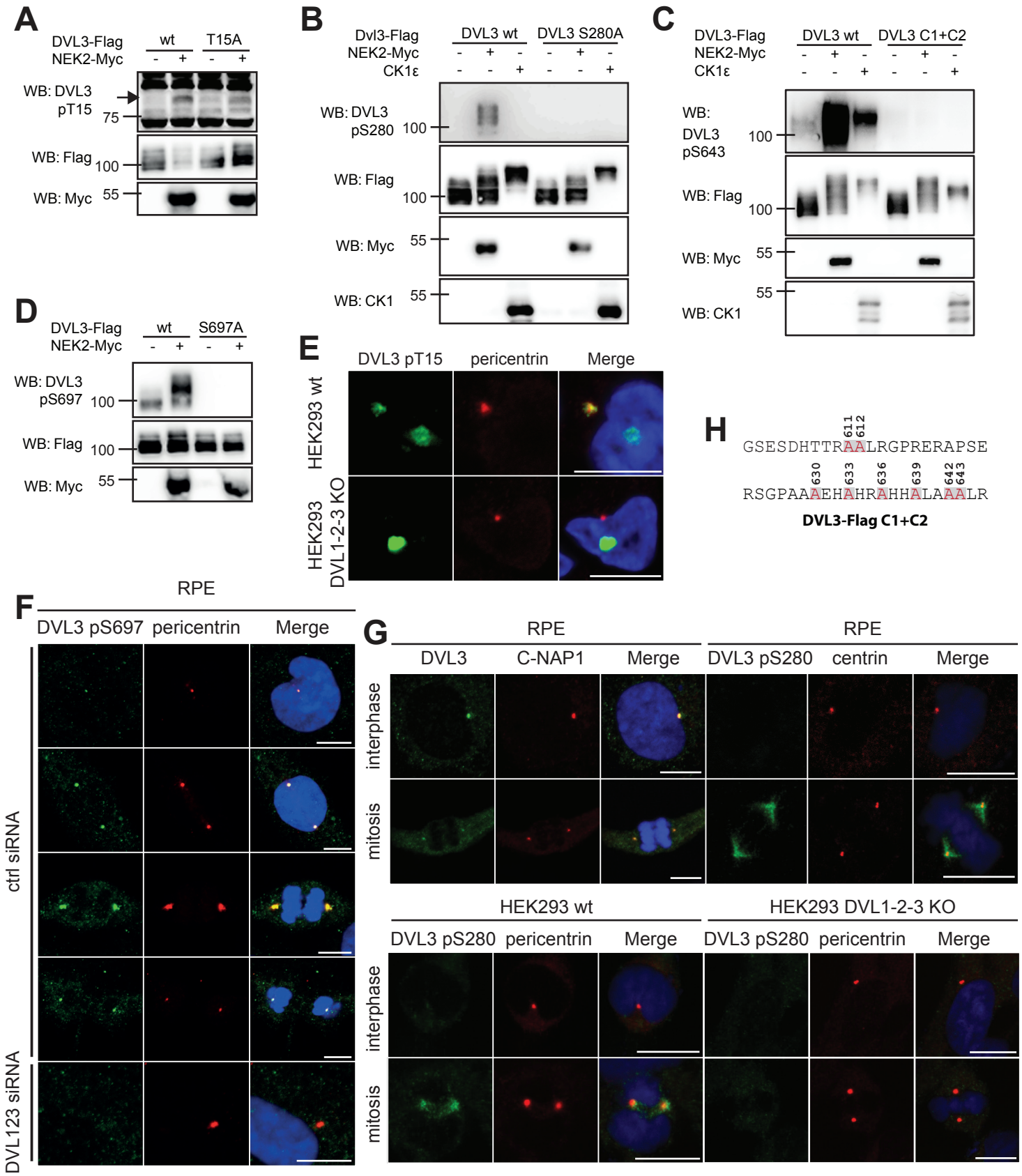

Figure S3. Characterization of novel phospho-DVL3-specific antibodies. HEK293 cells were co-transfected with NEK2 together with either wild-type DVL3 or constructs with corresponding alanine mutations and probed with (A) pT15 (B) pS280 phospho-specific antibody and (C) antibody recognizing epitope flanking pS643 of DVL3 and (D) pS697 phospho-specific antibody. Flag, Myc and CK1ε serve as input controls. All tested antibodies are specific and exhibit increased staining after NEK2 co-expression. (E) Antibody raised against pT15-DVL3 (green) co-localizes with pericentrin in HEK293 cells but not in HEK293 DVL1-2-3 KO cells. It should be noted that pT15-DVL3 antibody shows unspecific nuclear staining. (F) Antibody raised against p697-DVL3 (green) co-localizes with pericentrin and seems to accumulate in RPE cells at the centrosome during the progression of cell cycle. Centrosomal signal disappears after DVL1-2-3 siRNA. (G) Centrosomal DVL3 (green) shows weaker staining during mitosis than during interphase. Antibody raised against pS280-DVL3 recognizes DVL3 (green) only at the centrosome and mitotic spindles during mitosis, but not throughout the interphase in RPE and HEK293 cells. HEK293 DVL1-2-3 KO cells do not show any staining during interphase or mitosis. (H) Scheme depicting DVL3 constructs harboring alanine mutations in C-terminal part of the protein. DAPI (blue), scale bars: 10 μm.

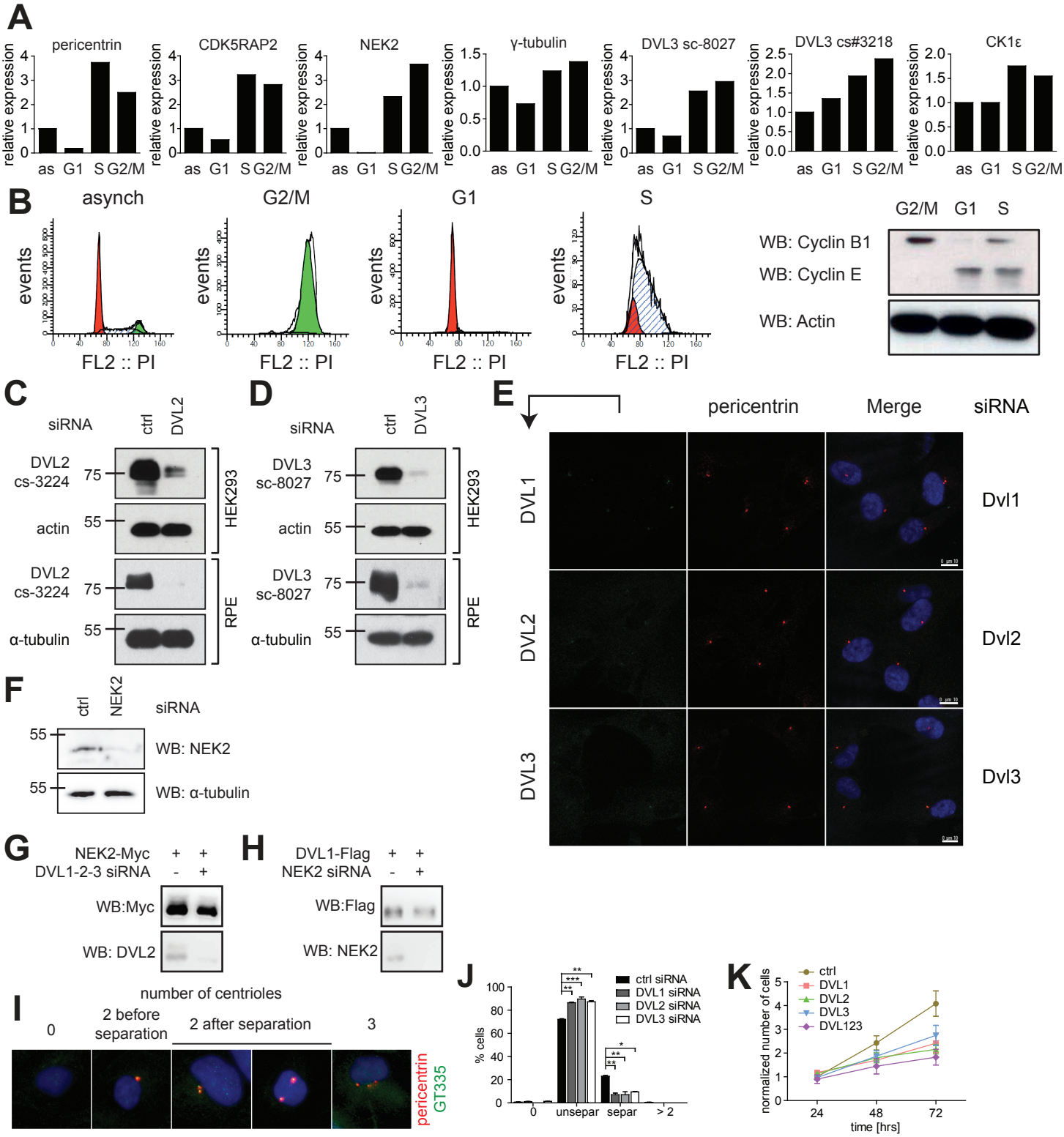

Figure S4. Control experiments for functional experiments shown in Fig. 3. (A) Western blotting quantification of protein expression during individual cell cycle stages as depicted in Fig. 2A (as - asynchronous). (B) Flow cytometry and WB controls for HeLa Fucci cells sorted according to cell cycle phases. (C, D) Validation of siRNA knockdown of (C) DVL2 and (D) DVL3 proteins in HEK293 and RPE cell lines. (E) RPE cells were transfected by siRNA against individual DVL isoforms, loss of specific centrosomal signal after siRNA mediated knock-down was visualized by immunofluorescence. (F) Validation of siRNA knockdown of NEK2 in RPE cells. (G, H) HEK293 cells were transfected with (G) DVL siRNA and NEK2 expression vector or (H) NEK2siRNA and DVL expression vector and analyzed by Western blotting. Individual siRNA do not exhibit cross-reactivity or influence expression of other proteins. (I) Overview of categories for centrosomal signals. One signal corresponds to a single interphase centrosome, or two centrosomes tightly linked with proteinaceous linker. Two close signals correspond to centrosomes at the onset of separation. Two distant signals represent cells at the onset of spindle formation. (J) RPE cells were transfected with control siRNA or siRNA against individual DVL isoforms. RPE cells were fixed and stained with anti-pericentrin and anti-glutamylated tubulin antibody and distribution of centrosomal signals was assessed (according to Figure S4I). Cells transfected with siRNA against individual DVL show increased proportion of centrosomes before separation and reduced proportion of separated centrosomes compared to ctrl siRNA. (K) Cells transfected with siRNA against individual DVL or all DVL isoforms (DVL1-2-3) show significantly reduced proliferation 72 hours, synergistic effect of compound DVL knockdown is shown. HEK 293 wt and DVL1-2-3 KO fixed, stained and characterized for parameters connected to cell cycle and centrosomes. Graphs represent mean ± SEM of two (J) and three (K) independent replicates. * P < 0.05; ** P < 0.01; *** P < 0.001; (ANOVA - Bonferroni's posttest). DAPI (blue), scale bars: 10 μm.

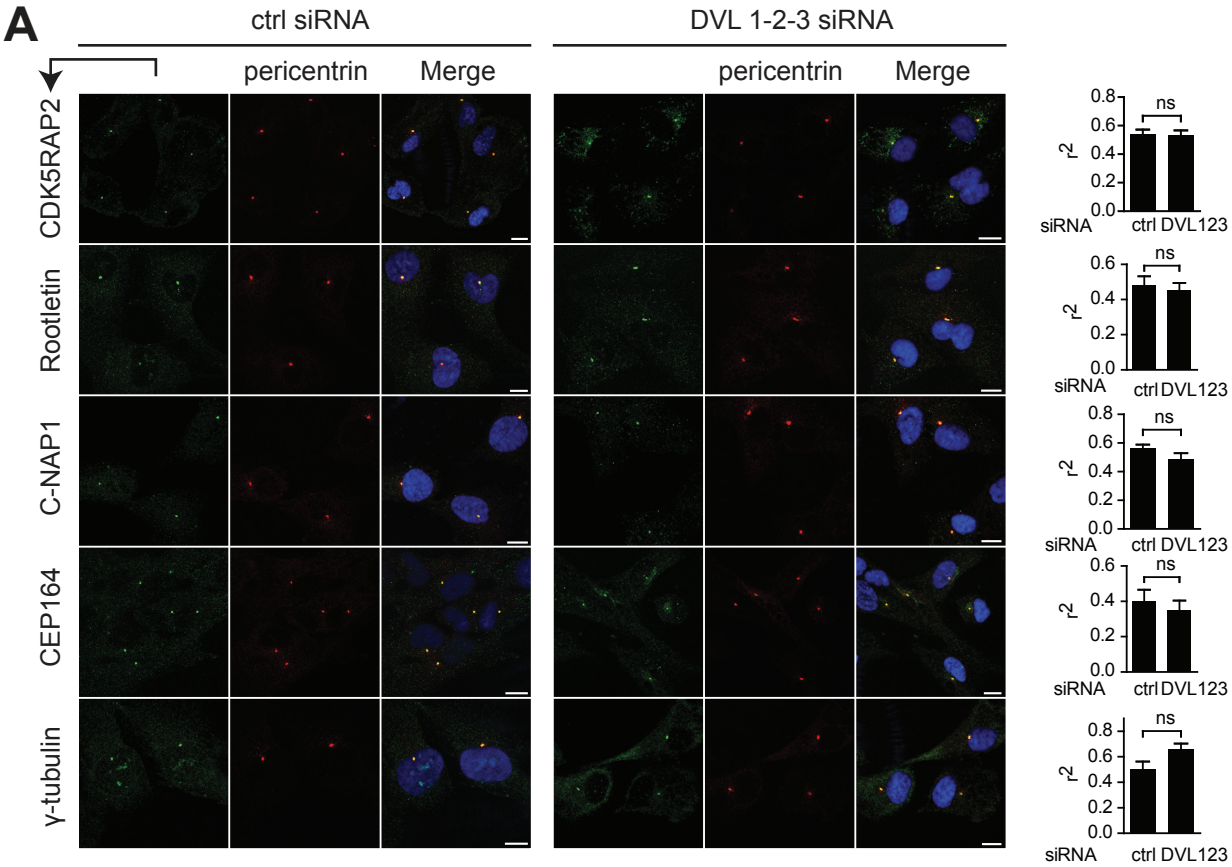
A
ctrl siRNA
DVL 1-2-3 siRNA
pericentrin
Merge
CDK5RAP2
Rootletin
C-NAP1
CEP164
γ-tubulin
r2
siRNA
ctrl DVL123
ns

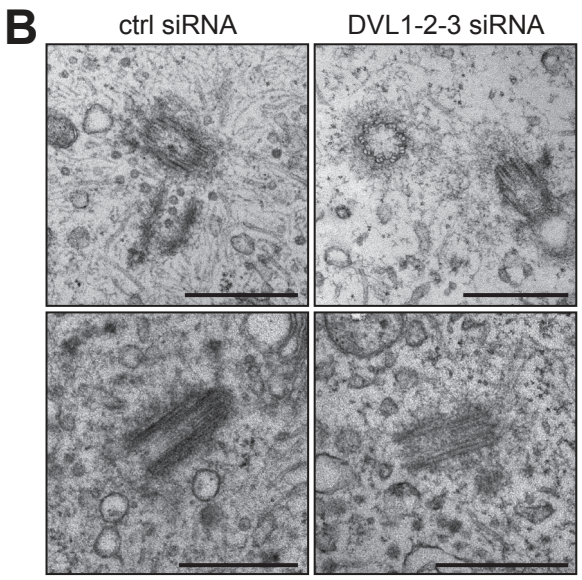
B
ctrl siRNA
DVL1-2-3 siRNA

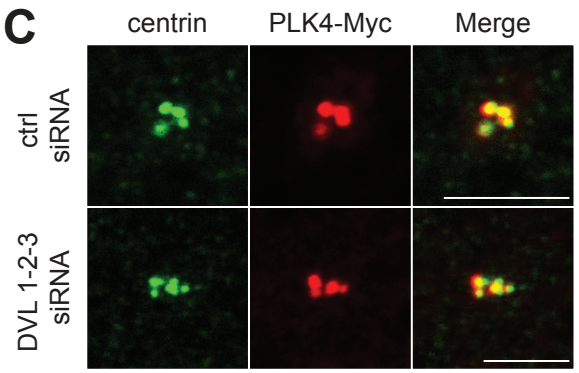
C
centrin
PLK4-Myc
Merge
ctrl siRNA
DVL 1-2-3 siRNA

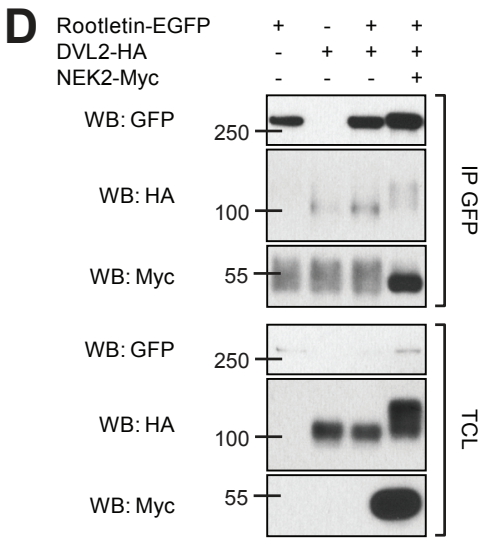
D
Rootletin-EGFP
DVL2-HA
NEK2-Myc
WB: GFP
WB: HA
WB: Myc
250
100
55
IP GFP
TCL

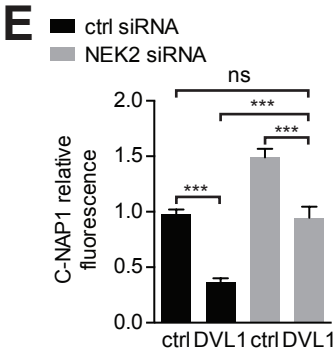
E
ctrl siRNA
NEK2 siRNA
C-NAP1 relative fluorescence
ctrl DVL1 ctrl DVL1
ns
***

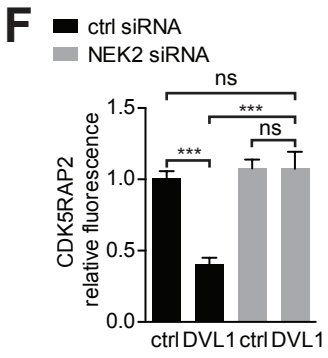
F
ctrl siRNA
NEK2 siRNA
CDK5RAP2 relative fluorescence
ctrl DVL1 ctrl DVL1
ns
***

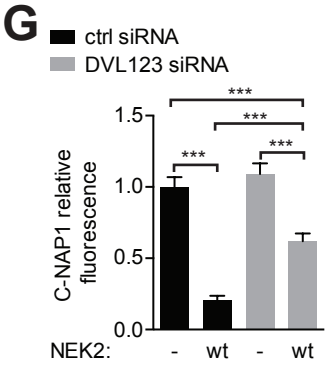
G
ctrl siRNA
DVL123 siRNA
C-NAP1 relative fluorescence
NEK2: - wt - wt
***

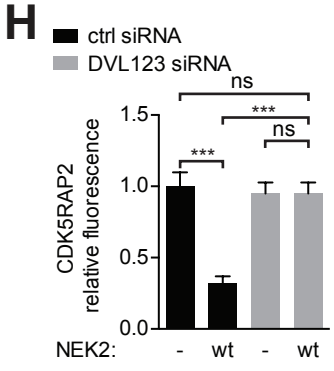
H
ctrl siRNA
DVL123 siRNA
CDK5RAP2 relative fluorescence
NEK2: - wt - wt
ns
***

Figure S5. Effects of DVL1-2-3 siRNA in RPE cells. (A) RPE cells were transfected with control or DVL1-2-3 siRNA and change of localization of centrosomal proteins was observed by confocal microscopy. DVL knockdown does not disturb localization of centrosomal proteins as assessed by comparing co-localization coefficients. (B) Ultrastructre of centrosomes visualized by electron microscope. RPE cells with depleted DVL show mostly undisturbed microtubule structure and composition. (C) RPE cells were transfected with control and DVL1-2-3 siRNA as described and after 24h PLK4 kinase (red) was co-transfected to induce centriole formation. Neither condition shows impaired ability to activate pathway for duplicating centrioles. (D) Rootletin does not co-immunoprecipitate with DVL2 in the absence or presence of NEK2 in HEK293 cells. (E, F) Expanded graphs for Figure 3 (B, C respectively) show changes in centrosomal C-NAP1 and CDK5RAP2 intensity after DVL1 overexpression in the absence or presence of NEK2. (G, H) Expanded graphs for Figure 3 (D, E respectively) show changes in centrosomal C-NAP1 and CDK5RAP2 intensity after NEK2 overexpression in the absence or presence of DVL. Graphs represent mean ± SEM of at least three independent replicates. * $P < 0.05$; ** $P < 0.01$; *** $P < 0.001$; (Student t-test – A; ANOVA - Bonferroni's posttest – E - H). DAPI (blue), scale bars: (B) 0,5 μm (C) 5 μm, (A) 10 μm.

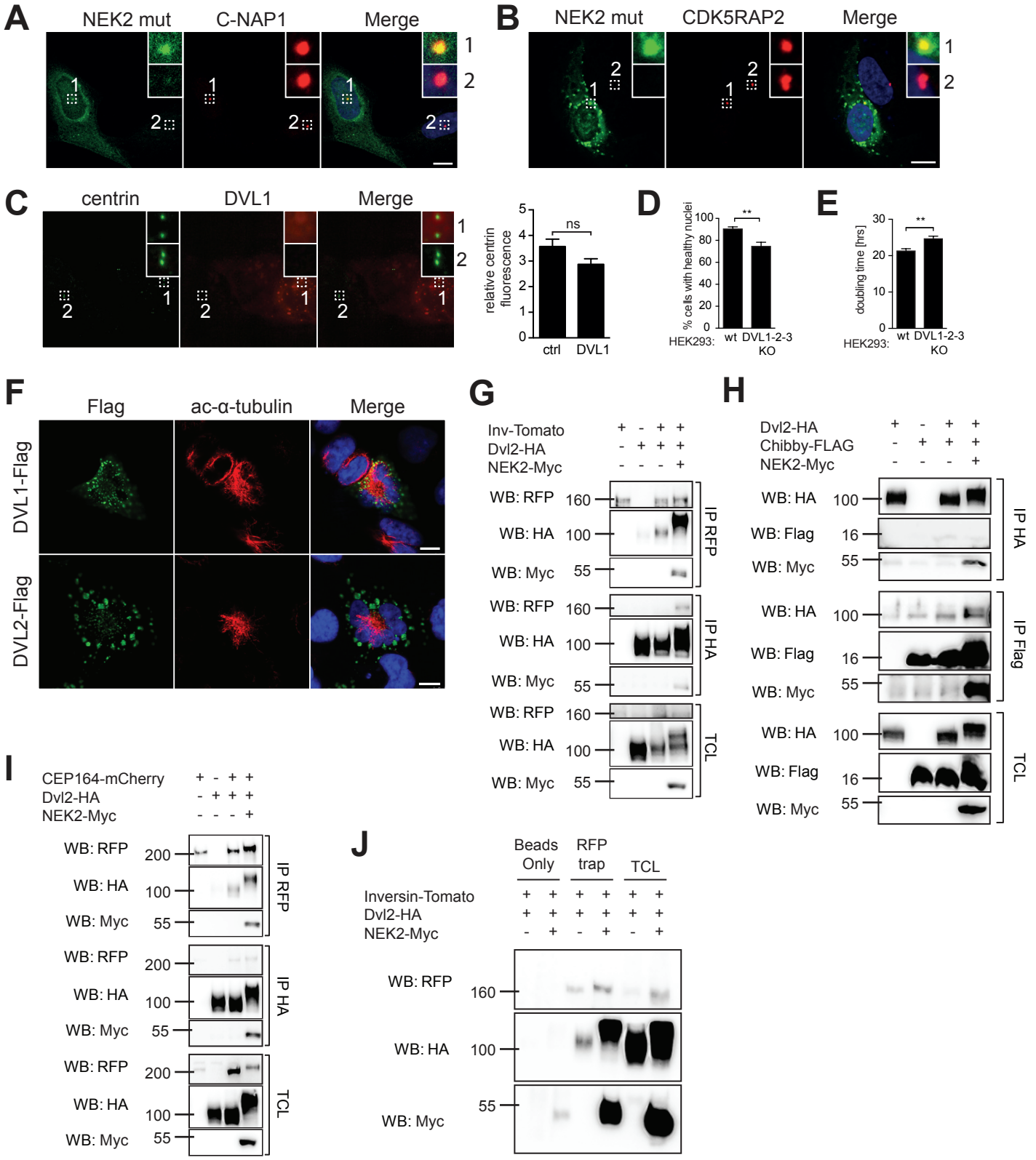

Figure S6. The effect of DVL/NEK2 on centrosomes and centrosomal proteins. (A, B) RPE cells were transfected with kinase inactive NEK2 (green). Centrosomal signal (red) of linker proteins C-NAP1 (A) and CDK5RAP2 (B) in transfected and untrasfected cells was quantified using fluorescence microscopy. Data are quantified in Fig. 3D-E. (C) DVL1 overexpression does not significantly displace centrin from centrosome in RPE cells (D) HEK293 DVL1-2-3 KO cells show decreased proportion of round healthy looking nuclei and (E) increased doubling time when compared to wild-type HEK293 cells. (F) Full-length DVL isoforms (DVL1, DVL2) (green) can induce phenotype arising from monopolar spindle formation. (G-I) Indicated proteins were overexpressed in HEK293 cells and immunoprecipitated as indicated and the presence of individual proteins in the pulldown was assessed by Western blotting. Ciliary protein Chibby does not co-immunoprecipitate with DVL2 in the absence or presence of NEK2 in HEK293 cells; binding of DVL2 to CEP164 is not increased after NEK co-expression unlike binding to Inversin (Inv). (J) Negative control for Fig. 3C,D and Fig. S6D-F. DVL phosphorylated by NEK2 does not non-specifically bind to control affinity beads. Graphs represent mean ± SEM of at least three independent replicates. * P < 0.05; ** P < 0.01; *** P < 0.001; (Student t-test – C, D, E). DAPI (blue), scale bars: 10 μm.

Supplementary Tables

Table S1. Amino acid residues phosphorylated by NEK2 as identified by mass spectrometry. NEK2-induced phosphorylations were scored based on a given criteria: number of identified phosphorylation instances was divided by total number of experiments. As NEK2 induced phosphorylations were considered qualitative changes and those phosphorylations that had ratio of %NEK2 to %ctrl higher than 3 - (%NEK2) / (%ctrl) > 3.

Dishevelled2			Dishevelled3		
AA	% ctrl (n=8)	% NEK2 (n=4)	AA	% ctrl (n=15)	% NEK2 (n=5)
S4	0.00	0.50	**T15**	0,00	0,20
T6	0.00	0.50	**S41**	0,00	0,20
S59	0.00	0.50	**T106**	0,00	0,40
S87	0.00	0.50	**S112**	0,00	0,40
S91	0.13	0.75	**S140**	0,13	0,40
S92	0.13	0.50	**S176**	0,00	0,20
S126	0.13	0.50	**T186**	0,07	0,20
S131	0.00	0.25	**T205**	0,20	0,60
S135	0.13	0.75	**S208**	0,20	0,60
S169	0.00	0.50	**S211**	0,07	0,40
T216	0.00	0.25	**S232**	0,07	0,60
T269	0.00	0.25	**S233**	0,07	0,20
S281	0.25	1.00	**S241**	0,07	0,20
S381	0.00	0.25	**S263**	0,00	0,40
S383	0.00	0.25	**S268**	0,00	0,20
T403	0.00	0.25	**S280**	0,07	0,60
S406	0.13	0.75	**S350**	0,07	0,40
T427	0.00	0.25	**S386**	0,00	0,20
S435	0.00	0.75	**S394**	0,00	0,20
T448	0.00	0.50	**S407**	0,00	0,60
T496	0.00	0.25	**S410**	0,00	0,40
S514	0.00	0.25	**S421**	0,13	0,80
S520	0.00	0.25	**S469**	0,00	0,20
S552	0.00	0.25	**S505**	0,00	0,20
T575	0.00	0.25	**S559**	0,00	0,20
S591	0.13	0.50	**S564**	0,00	0,40
S597	0.00	0.25	**S566**	0,00	0,40
			S598	0,00	0,20
			S601	0,00	0,20
			S603	0,07	0,20
			S612	0,13	0,80
			S630	0,00	0,40
			S636	0,00	0,40
			S639	0,20	0,60
			S642	0,00	0,40
			S643	0,20	0,80
			S652	0,00	0,20
			S689	0,13	0,40
			T695	0,00	0,40
			S697	0,13	0,60
			S700	0,13	0,40

Table S2.

Amino acid residues phosphorylated by NEK2 as identified by mass spectrometry. NEK2-induced phosphorylations were scored based on a given criteria: number of identified phosphorylation instances was divided by total number of experiments. As NEK2 induced phosphorylations were considered qualitative changes and those phosphorylations that had ratio of %NEK2 to %ctrl higher than 3. Difference in phosphorylations between DVL wt/ko HEK293 cells was scored followingly: cutoff was introduced not to take rare, problematically detectable events into consideration. Cutoff was set as 1/100 of maximal response. Only phosphorylation events above cutoff that show different phosphorylation pattern in DVL wt and KO cells are marked yes.

C-NAP1				CDK5RAP2			
AA	% ctrl (n=2)	% NEK2 (n=2)	Diff. between DVL wt/KO	AA	% ctrl (n=4)	% NEK2 (n=4)	Diff. between DVL wt/KO
S15	0	0,5	no	**S16**	0	0,25	no
S38	0	0,5	no	**S111**	0	0,25	no
T54	0	1	no	**S132**	0	1	no
S157	0	1	no	**S139**	0	1	no
S196	0	1	no	**S193**	0	0,5	no
S213	0	0,5	no	**S199**	0	1	no
T224	0	1	no	**T212**	0	0,25	no
S229	0	0,5	no	**S228**	0	1	no
S235	0	1	no	**S254**	0	1	no
T253	0	1	no	**S255**	0	1	no
S272	0	1	no	**S262**	0	0,25	no
T293	0	0,5	no	**T264**	0	0,75	no
S295	0	1	no	**S343**	0	1	no
S329	0	1	no	**T344**	0	1	no
S331	0	1	no	**T433**	0	0,25	no
S340	0	1	no	**S461**	0	1	no
T389	0	1	no	**S466**	0	0,25	no
S393	0	1	no	**S479**	0	0,75	no
T441	0	0,5	no	**T481**	0	0,5	no
S460	0	1	no	**S483**	0	1	no
S502	0	0,5	no	**S518**	0	0,5	no
S538	0	1	no	**S527**	0	1	no
S552	0	0,5	yes	**S538**	0	0,5	no
S576	0	0,5	no	**T566**	0	0,5	no
S582	0	0,5	no	**T569**	0	0,5	no
S583	0	1	no	**S571**	0	0,25	no
S699	0	1	no	**S608**	0	0,5	no
S763	0	1	no	**S612**	0	0,25	no
S764	0	1	no	**S622**	0	0,25	no
S771	0	1	no	**S644**	0	0,25	no
S772	0	1	no	**S677**	0	0,75	no
S781	0	0,5	no	**S678**	0	0,5	no
T817	0	0,5	no	**S684**	0	1	no
S820	0	0,5	no	**T690**	0	0,25	no
S1025	0	0,5	yes	**S698**	0	1	no
T1040	0	1	no	**T704**	0	0,5	no

S1056	0	1	no	**S717**	0	0,5	no
T1058	0	1	no	**S724**	0	0,5	no
S1060	0	1	no	**Y731**	0	0,25	no
S1076	0	1	no	**S787**	0	1	no
S1131	0	0,5	no	**S817**	0	1	no
S1141	0	1	no	**S837**	0	1	no
S1204	0	0,5	yes	**S842**	0	1	no
S1281	0	1	no	**S844**	0	0,25	no
S1324	0	0,5	no	**S846**	0	0,5	no
S1372	0	0,5	no	**T861**	0	0,5	no
S1540	0	0,5	no	**T866**	0	0,5	no
S1609	0	0,5	no	**S871**	0	0,5	no
S1691	0	1	no	**S873**	0	0,5	no
S1774	0	1	no	**S890**	0	1	no
S1800	0	0,5	no	**S925**	0	0,5	no
S1927	0	1	no	**S1037**	0	1	no
S1949	0	1	no	**S1081**	0	0,5	no
S1952	0	0,5	no	**S1089**	0	0,5	no
S1991	0	1	no	**S1091**	0	0,5	no
S1993	0	1	no	**S1094**	0	0,5	no
T2000	0	0,5	no	**S1098**	0	1	no
S2004	0	1	no	**T1102**	0	0,5	no
S2064	0	1	no	**S1142**	0	0,5	no
S2095	0	1	no	**S1177**	0	0,5	no
S2128	0	0,5	no	**S1178**	0	0,5	no
S2138	0	1	no	**S1206**	0	1	no
T2183	0	0,5	no	**S1249**	0	0,5	no
S2186	0	1	no	**S1253**	0	1	no
S2189	0	0,5	no	**S1326**	0	0,5	no
S2200	0	1	no	**S1363**	0	0,5	no
S2206	0	1	no	**T1387**	0	0,25	no
T2233	0	0,5	no	**S1419**	0	1	no
S2234	0	1	no	**S1454**	0	0,5	no
T2235	0	0,5	no	**T1456**	0	0,5	no
S2240	0	0,5	no	**S1484**	0	0,25	no
S2267	0	1	no	**S1490**	0	1	no
S2287	0	0,5	no	**S1507**	0	0,5	no
S2298	0	1	no	**S1555**	0	0,5	no
T2299	0	1	no	**S1563**	0	1	no
S2332	0	0,5	no	**S1595**	0	0,25	no
T2364	0	1	no	**S1652**	0	0,5	no
T2380	0	0,5	no	**S1700**	0	0,5	no
S2381	0	1	no	**S1702**	0	0,5	no
S2390	0	0,5	no	**S1711**	0	1	no
S2417	0	1	no	**S1778**	0	0,25	no
S2421	0	1	no				

Table S3. Antibodies, plasmids and other reagents

Protein	Catalogue #	Manufacturer	**Application**
Pericentrin	ab4448	Abcam	WB, IF
Pericentrin	ab28144	Abcam	WB, IF
CDK5RAP2	ab70213	Abcam	WB, IF
Rootletin	NBP1-80820	Novus Biologicals	IF
CNAP	14498-1-AP	Proteintech	WB, IF
Centrin	04-1624	Millipore	IF
GT335		courtesy of Carsten Janke	IF
γ-tubulin	T5326	Sigma	WB
γ-tubulin	T5192	Sigma	IF
NEK2	sc-33167	SantaCruz	IP
NEK2	610593	BD Biosciences	WB, IF
CEP164	4533.00.02	sdix	IF
α-tubulin	T6199	Sigma	WB
acetylated-α-tubulin	#5335	Cell Signaling	IF
Cyclin-A	Sc-751	SantaCruz	WB
Cyclin-B1	ab72	Abcam	WB
Cyclin-E	sc-481	SantaCruz	WB
Dishevelled-1	sc-8025	SantaCruz	WB, IF
Dishevelled-2	sc-8026	SantaCruz	WB, IF
Dishevelled-2	sc-13974	SantaCruz	WB, IF
Dishevelled-2	#3216	Cell Signaling	WB
Dishevelled-2	#3224	Cell Signaling	WB
Dishevelled-3	sc-8027	SantaCruz	WB, IF
Dishevelled-3	#3218	Cell Signaling	WB, IP
pS643-Dishevelled-3		(1)	WB, IF
pT15-Dishevelled-3	prepared by immunizing rabbits by CLDGQE(Tp)PYLVK peptide. Immunizationand production of antibody was performed on a service basis by Moravian Biotechnology		WB, IF
pS280-Dishevelled-3	prepared by immunizing rabbits by CGIYIG(pS)IMKGGA peptide. Immunizationand production of antibody was performed on a service basis by Moravian Biotechnology		WB, IF
pS697-Dishevelled-3	prepared by immunizing rabbits by CPELTA(Sp)RQSFR peptide. Immunizationand production of antibody was performed on a service basis by Moravian Biotechnology		WB, IF
CK1ε	sc-6471	SantaCruz	WB
Flag	F1804	Sigma	WB, IF
Flag	F7425	Sigma	IP
Myc	C3956	Sigma	WB, IP
Myc	sc-40	SantaCruz	WB, IF
HA.11	MMS-101R	Covance	WB, IF
HA	ab9110	Abcam	IP
GFP	20R-GR-011	Fitzgerald	IP

GFP	MAB3580	Millipore	WB
RFP	5F8	Chromotek	WB
IgG	#3900	Cell Signaling	IP

Table S4.

Plasmid	Reference
DVL1-Flag	(2)
DVL1-YFP	courtesy of Stephane Angers
DVL2-Flag	(3)
DVL3-Flag	(4)
DVL3-Flag$^{87-716}$	(4)
DVL3-Flag$^{332-716}$	(4)
DVL3-Flag$^{1-246}$	(4)
DVL3-Flag$^{1-442}$	(4)
DVL3-Flag$^{1-495}$	(4)
DVL3-Flag S280A	(1)
DVL3-Flag C1+C2	(1)
DVL3-Flag T15A	obtained by site-directed mutagenesis of DVL3-Flag
DVL3-Flag S407A	obtained by site-directed mutagenesis of DVL3-Flag
DVL3-Flag S697A	obtained by site-directed mutagenesis of DVL3-Flag
DVL3-Flag M1 (F33S)	obtained by site-directed mutagenesis of DVL3-Flag
DVL2-HA	(5)
DVL2-HA M1 (F43S)	(5)
DVL3-HA	(6)
DVL2-GFP	(7)
NEK2wt-Myc	(8)
NEK2mut-Myc (K37R)	(8)
GFP-C2	Clonetech
hCK1ε	(9)
XCK1	(10)
PLK1-Flag	courtesy of Erich Nigg
PLK4-Myc	(11)
CEP164	(12)
Inversin	courtesy of Jeffrey D. Axelrod
Chibby	(13)
CDK5RAP2-Flag	(14)
Rootletin-EGFP	(15)
C-NAP1-EGFP	courtesy of Andrew Fry

Table S5.

siRNA	Sequence/Catalog No.	Manufacturer
control	#AM4636	Ambion
Dishevelled-1	GGAGGAGAUCUUUGAUGACdTdT	Eurogentec
Dishevelled-2	GGAAGAAAUUUCAGAUGACdTdT	Eurogentec
Dishevelled-3	GGAGGAGAUCUCGGAUGACdTdT	Eurogentec
NEK2	GGAAUGCCACAGACGAAGUdTdT	Eurogentec

Supplementary Materials and Methods

Mass spectrometry

Samples were loaded onto SDS-PAGE gels, separated, fixed with acetic acid in methanol, stained with Coomasie brilliant blue for 1 hour and partially destained.

Corresponding 1-D bands were excised. After destaining, the proteins in gel pieces were incubated with 10mM DTT at 56°C for 45 min. After removal of DTT excess samples were incubated with 55mM IAA at room temperature in darkness for 30 min, then alkylation solution was removed and gel pieces were hydrated for 45 min at 4 °C in digestion solution (5 ng/µl trypsin, sequencing grade, Promega, Fitchburg, Wisconsin, USA, in 25mM AB). The trypsin digestion proceeded for 2 hours at 40°C on Thermomixer (750 rpm; Eppendorf, Hamburg, Germany). Subsequently, the tryptic digests were subsequently cleaved by chymotrypsin (5 ng/µl, sequencing grade, Roche, Basel, Switzerland, in 25mM AB) for 2 hours at 30 °C. Digested peptides were extracted from gels using 50% ACN solution with 2.5% formic acid and concentrated in speedVac concentrator (Eppendorf, Hamburg, Germany).

The aliquot (1/10) of concentrated sample was directly analyzed by LC-MS/MS for protein identification. The rest of sample was used for phosphopeptide analysis. Sample was diluted with acidified acetonitrile solution (80% ACN, 2% FA). Phosphopeptides were enriched using Pierce Magnetic Titanium Dioxide Phosphopeptide Enrichment Kit (Thermo Scientific, Waltham, Massachusetts, USA) according to manufacturer protocol. Eluates were concentrated under vacuum and then diluted in 10 µl of 0.1% FA solution before LC-MS/MS analysis.

Liquid chromatography-tandem mass spectrometry (LC–MS/MS) analysis was performed using reverse phase RSLCnano system (Dionex, Sunnyvale, CA, USA) on-line coupled with an Orbitrap Elite Hybrid Spectrometer equipped by ETD fragmentation (Thermo Fisher Scientific, Waltham, MA). Before LC separation, tryptic digests were on-line-concentrated and desalted using trapping column (100 µm x 30 mm) filled with 3.5-µm X-Bridge BEH 130 C18 sorbent (Waters). After washing of the trapping column with 0.1% FA, the peptides were eluted (300 nl/min) from the trapping column onto an Acclaim Pepmap RSLC C18 column (2 µm particles, 75 µm x 250 mm; Thermo Fisher Scientific) by the following gradient program (mobile phase A, 0.1% FA in water; mobile phase B, acetonitrile: methanol:2,2,2-trifluoroethanol (6:3:1; v/v/v) containing 0.1% FA); the gradient elution started at 2% mobile phase B and increased from 2% to 45% during the first 90 min (11% in the 30 min, 25% in the 60 min, and 45% in 90 min), then increased linearly to 95% of mobile phase B in the next 5 min and remained at this state for the next 15 min. The analytical column outlet was directly connected to the Nanospray Flex Ion Source (Thermo Fisher Scientific). MS data were acquired in a data-dependent strategy selecting up to top 10 precursors based on precursor abundance in the survey scan (350–1700 m/z). Mass spectrometer was operating in the positive ion mode with collision-induced dissociation followed; in case of neutral loss detection (32.7, 49.0, 65.3, and 98; with m/z tolerance of -1.5 and +0.5

Da) ETD fragmentation with supplemental activation (energy 20, arbitrary units) was triggered. The resolution of the survey scan was 120,000 (400m/z) with a target value of 1.106 ions, 1 microscan, and a maximum injection time of 200 ms. Low resolution collision-induced dissociation or ETD MS/MS spectra were acquired with a target value of 10,000 ions in rapid scan mode with the m/z range adjusted according to actual precursor mass and charge. MS/MS acquisition in the linear ion trap was carried out in parallel to the survey scan in the Orbitrap analyzer by using the preview mode. The maximum injection time forMS/MS was 50 ms. ETD reaction time was 100 ms (double-charged precursors, adjusted according to charge state). Dynamic exclusion was enabled for 45 s after one MS/MS spectra acquisition, and early expiration was disabled. The isolation window for MS/MS fragmentation was set to 2 m/z. The data were searched with MASCOT (Version 2.2 or higher, Matrix Science, Boston, MA) against NCBInr database (non-redundant, taxonomic restriction Mammalia) with settings corresponding to trypsin/chymotrypsin specificity (two miss-cleavages allowed) and optional modifications: oxidation (M), carbamidomethylation (C), phosphorylation (Ser, Thr, Tyr). Mass tolerances for peptides and MS/MS fragments were 5 ppm and 0.5 Da, respectively. The significance threshold was set to $p < 0.01$. The phosphoRS feature was used for phosphorylation localization. All phosphorylation sites were manually confirmed in profile MS/MS spectra when necessary.

Determination of doubling time

HEK293 wt and DVL1-2-3 KO cells were split every 48h at density $1x10^6$ cells on 10 cm dish for two weeks prior to expriment to exclude effects of previous passaging. Subsequently, cells were trypsinzed every 48 hours, counted and split at density $1x10^6$ cells on 10 cm dish for three weeks. Doubling time was calculated according to formula:

$$t_d = \frac{t * \log 2}{\log n_{end} - \log n_{start}}$$

t – duration of experiment
n_{end} – final amount of cells
n_{start} – initial amount of cells

Image analysis and quantification

For centrosome counts after siRNA treatment, RPE cells were stained with pericentrin antibody, and at least 200 cells were counted and scored for different centrosomal patterns (Fig.S4G). For monopolar spindle defect, HEK293 cells were stained with Flag/HA and acetylated-α-tubulin antibody. At least 150 cells were counted and scored per condition. For DVL localization change, wt and mut NEK2-Myc or empty vector was co-expressed, and at least 200 cells were counted and scored for punctate or even appearance of DVL in cytoplasm. For assessment of nuclei in HEK293 wt and DVL1-2-3 KO cells at least 200 cells were counted and scored for aberrant nuclear shapes such as multilobular or crescent-shaped. For relocalization of centrin and centrosomal linker proteins after DVL1-Flag or NEK2-Myc co-expression and relocalization of DVL after NEK2-Myc co-expression, images of at least 10 transfected or non-transfected cells were taken from each condition at identical settings. Background from images was subtracted equally to remove cytoplasmic staining of centrosomal proteins. Amount of signal for individual linker proteins was quantified by ImageJ, and levels for one replicate were normalized to the average value all untransfected control siRNA measurements. Co-localization of centrosomal proteins was quantified by ImageJ using Coloc2 plugin. Pearson correlation was inferred from of at least three independent measurements, coefficient of determination (R^2) was computed, plotted and analyzed statistically (Fig.1C, Fig.2E-F).

Transmission electron microscopy (TEM)

Cells were fixed with 300 mmol/l glutaraldehyde in 100 mmol/l cacodylate buffer and postfixed in 40 mmol/l osmium tetroxide in 100 mmol/l cacodylate buffer. Cell suspension was embedded into agar blocks, these were dehydrated in ethanol and embedded in araldite resin (Durcupan ACM, Fluka). Thin sections (60-90 nm) were made on Leica EM UC 6 ultramicrotome. After staining with 2% uranyl acetate and 1% lead citrate, sections were examined in transmission electron microscope FEI Morgagni 268D (FEI Company, The Netherlands).

Co-immunoprecipitation

Cells were lysed in cold lysis buffer supplemented with protease inhibitors (Roche, 11836145001), phosphatase inhibitors (Calbiochem, 524625), 0.1mM DTT. Lysate was collected after 20 minutes of lysis at 4 ^{o}C, and was cleared by centrifugation at 16.1 RCF for 20 minutes. Samples were incubated with the antibody for 40 minutes, then 30µl of G protein sepharose beads (GE healthcare, 17-0618-05) equilibrated in the lysis buffer were added to each sample. Samples were incubated on the carousel overnight, washed 3 times with lysis buffer, 40 µl of 2x Laemmli buffer was added, samples were boiled and subjected to analysis by Western blotting.

Dual luciferase assay

For the luciferase reporter assay, cells were transfected with 0.1 µg of Super8X TopFlash construct and 0.1 µg of *Renilla* luciferase construct per well in a 24-well plate 24 h after seeding. For the TopFlash assay, a Promega Dual-Luciferase assay kit was used according to the manufacturer's instructions. Relative luciferase units were measured on a MLX luminometer (Dynex Technologies) and normalized to the *Renilla* luciferase expression 24 h post-transfection. Results were shown as the means with SEM of three independent experiments.

***In vitro* kinase assay**

Following N-terminally GST-tagged constructs were generated for in vitro kinase assay: Dvl3-DIX (aa 1-82), Dvl3-PDZ (aa 249-321) and Dvl3-DEP-C (aa 422-716). Assay was performed according to following protocol: 10 µM ATP, 50 ng of substrate and 200 ng of recombinant NEK2 kinase (Invitrogen) was incubated in reaction buffer (50 mM Tris (pH 7.4), 0.1 mM EGTA, 10 mM $MgCl_2$, 1x Protease Inhibitor Coctail Tablets (Roche), 1x Phosphatase Inhibitor Coctail Set II (Merck), 0.01 M N-ethylmaleimide) at 30 °C for 60 min. To terminate the reaction, samples were mixed with 5x Laemmli buffer, boiled at 95 °C for 5 min, subjected to SDS-PAGE and analysed by Mass spectrometry

Centrosome purification

Near-confluent HEK293 cells were treated with Nocodazole (10µg/ml) and Cytochalasin B (5µg/ml) for 90 min. Plates were washed successively with following buffers (i) PBS, (ii) 8% Sucrose in 0,1x PBS, (iii) 8% Sucrose in ddH_20 (iv) 1 mM Tris, pH 8,0; 8 mM 2-mercaptoethanol. Plates were immediately lysed in lysis buffer (1 mM Tris, pH to 8.0 with HCl; 0.5% NP-40; before use, 8 mM 2-mercaptoethanol and protease inhibitors) at 4°C for 30 min and supplemented with PE buffer (100 mM PIPES, pH to 7.2 with KOH; 10 mM EDTA). Lysates were centrifuged at 1500g for 3 min at 4°C. Supernatant was collected, underlaid with Ficoll cushion (20% Ficoll (Sigma) (w/w) in 1× PE, 0.1% NP-40) and centrifuged at 25000g for 15 min at 4°C. Layer above Ficoll cushion was collected and analyzed for presence of centrosomes by western blotting.

Generation of DVL1, DVL2, DVL3 triple knockout cells by Crispr/Cas

Guide RNA Sequences targeting DVL1/2 or DVL3 were cloned into px330 (Addgene #42230) following plasmid supplier's protocol. Hek293T cells were transfected with both px330 constructs and single cell clones were isolated via limited dilution. Clones were screened with PCR amplification, followed by TA cloning using pGEM-T easy vector kit (Promega), followed by Sanger sequencing mini-prepped (Invitrogen) colonies.

Following primers were used:

DVL1/2 gRNA Forward:	5' caccGCTACATTGGCTCCATCATGA 3'
DVL1/2 gRNA Reverse:	5' aaacTCATGATGGAGCCAATGTAGC 3'
DVL3 gRNA Forward:	5' caccGACCATGCTTCAATGGCCGGG 3'
DVL3 gRNA Reverse:	5' aaacCCCGGCCATTGAAGCATGGTC 3'
DVL1 Genotyping PCR Forward:	5' GGCATCGTCATTGCTCATGT 3'
DVL1 Genotyping PCR Reverse:	5' GACAGTCTGTTCCCAGGCTC 3'
DVL2 Genotyping PCR Forward:	5' GCGTCATCGTTGCTCATGTT 3'
DVL2 Genotyping PCR Reverse:	5' AGGGTGAGGGGTTCCTACAG 3'
DVL3 Genotyping PCR Forward:	5' GCCCAGGAGAGTCATGTTGG 3'
DVL3 Genotyping PCR Reverse:	5' AGCAAGGCATGAAGGCCTAA 3'

References

1. Bernatik O*, et al.* (2014) Functional analysis of dishevelled-3 phosphorylation identifies distinct mechanisms driven by casein kinase 1 and frizzled5. *J Biol Chem* 289(34):23520-23533.
2. Tauriello DV*, et al.* (2010) Loss of the tumor suppressor CYLD enhances Wnt/beta-catenin signaling through K63-linked ubiquitination of Dvl. *Mol Cell* 37(5):607-619.
3. Narimatsu M*, et al.* (2009) Regulation of planar cell polarity by Smurf ubiquitin ligases. *Cell* 137(2):295-307.
4. Angers S*, et al.* (2006) The KLHL12-Cullin-3 ubiquitin ligase negatively regulates the Wnt-beta-catenin pathway by targeting Dishevelled for degradation. *Nat Cell Biol* 8(4):348-357.
5. Schwarz-Romond T*, et al.* (2007) The DIX domain of Dishevelled confers Wnt signaling by dynamic polymerization. *Nat Struct Mol Biol* 14(6):484-492.
6. Ma L, Wang Y, Malbon CC, & Wang HY (2010) Dishevelled-3 C-terminal His single amino acid repeats are obligate for Wnt5a activation of non-canonical signaling. *Journal of molecular signaling* 5:19.
7. Chen W*, et al.* (2003) Dishevelled 2 recruits beta-arrestin 2 to mediate Wnt5A-stimulated endocytosis of Frizzled 4. *Science* 301(5638):1391-1394.
8. Fry AM, Meraldi P, & Nigg EA (1998) A centrosomal function for the human Nek2 protein kinase, a member of the NIMA family of cell cycle regulators. *EMBO J* 17(2):470-481.
9. Foldynova-Trantirkova S*, et al.* (2010) Breast cancer-specific mutations in CK1epsilon inhibit Wnt/beta-catenin and activate the Wnt/Rac1/JNK and NFAT pathways to decrease cell adhesion and promote cell migration. *Breast cancer research : BCR* 12(3):R30.
10. Peters JM, McKay RM, McKay JP, & Graff JM (1999) Casein kinase I transduces Wnt signals. *Nature* 401(6751):345-350.
11. Habedanck R, Stierhof YD, Wilkinson CJ, & Nigg EA (2005) The Polo kinase Plk4 functions in centriole duplication. *Nat Cell Biol* 7(11):1140-1146.
12. Chaki M*, et al.* (2012) Exome capture reveals ZNF423 and CEP164 mutations, linking renal ciliopathies to DNA damage response signaling. *Cell* 150(3):533-548.

13. Takemaru K*, et al.* (2003) Chibby, a nuclear beta-catenin-associated antagonist of the Wnt/Wingless pathway. *Nature* 422(6934):905-909.
14. Buchman JJ*, et al.* (2010) Cdk5rap2 interacts with pericentrin to maintain the neural progenitor pool in the developing neocortex. *Neuron* 66(3):386-402.
15. Bahe S, Stierhof YD, Wilkinson CJ, Leiss F, & Nigg EA (2005) Rootletin forms centriole-associated filaments and functions in centrosome cohesion. *J Cell Biol* 171(1):27-33.